Light-hole contribution to noise and diffusion in *p*-type germanium at low temperatures

V. Mitin* and C. M. Van Vliet
Centre de Recherches Mathématiques, Université de Montréal, CP 6128-A, Montréal (QC), Canada H3C 3J7
(Received 30 May 1989)

The aim of this paper is to investigate noise and diffusion for fields that show the diffusion-to-streaming transition. A Monte Carlo (MC) computation of the drift velocity, mean energy, diffusion constant, and of the velocity-velocity correlation function $C(\tau)$ is presented for *p*-type germanium at low temperatures (≤ 4 K). Analytical results for streaming are reviewed. The MC computations for the case that only heavy holes are involved, in the presence of acoustical-phonon scattering and impurity scattering, in addition to the optical-phonon emission responsible for streaming, indicate that $C(\tau)$ damps out for large τ; the diffusivities $D_\perp$ and $D_\parallel$ are in agreement with previous results. However, the MC computations when the contribution of the light holes is included (not considered before), involving the movement of two species as well as interband transitions, show that the streaming behavior and the associated diffusion coefficient are very substantially changed from the one-band results. The $D_\parallel$ is dominated by transitions, and $C(\tau)$ shows quasiperiodicity with about one-third of the heavy-holes streaming period, i.e., $\simeq \tau_0/3$.

I. INTRODUCTION

In recent years streaming motion and related phenomena have been studied in much detail.[1-3] Streaming motion can be realized at low temperatures when there is almost no scattering, except scattering involving optical-phonon emission. In ideal streaming motion a carrier is accelerated by the electric field in the "passive region," $\mathcal{E} < \hbar\omega_0$, up to the energy $\mathcal{E} \approx \hbar\omega_0$ ($\mathcal{E}$ is the kinetic energy and ω_0 is the optical-phonon frequency), after which an optical phonon is emitted; the electron then returns to the state $\mathcal{E} \approx 0$, after which it is again accelerated to the energy $\hbar\omega_0$, and the emission is repeated. To observe this effect, certain conditions must be fulfilled.

(1) The temperature must be low enough, generally

$$kT \ll \hbar\omega_0 , \tag{1}$$

so that absorption of optical phonons is negligible, their number being too small.

(2) The semiconductor must be characterized by a strong optical-phonon coupling constant (or polar-optical-phonon constant as the case may be), such as in *p*-type Ge, *n*-type InSb, AgCl, AgBr, and other materials, so that when the carrier penetrates into the "active region" $\mathcal{E} \geq \hbar\omega_0$, the probability to emit an optical (or polar-optical) phonon exceeds the probabilities for other scattering mechanisms by at least one order of magnitude.

(3) There must be an electric field region $F^- < F < F^+$ commensurate with the acceleration process for streaming to occur, where, with m^* and e being the effective mass and absolute charge,

$$F^- \simeq (2\hbar\omega_0 m^*/e^2)^{1/2}(1/\tau_{\rm imp} + 1/\tau_{\rm ac}) \tag{2}$$

is the lower limit and

$$F^+ \simeq (2\hbar\omega_0 m^*/e^2)^{1/2}\mathcal{A}/10.3 \tag{3}$$

is the upper limit. Here $\tau_{\rm imp}$ and $\tau_{\rm ac}$ are the averages in the passive region of the relaxation times for impurity and acoustical-phonon scattering, respectively; note $F^- \to 0$ if these scattering processes are absent. Further, $\mathcal{A}^{-1}$ is the scaled reciprocal optical-phonon relaxation time, i.e., $1/\tau_{\rm op} = \mathcal{A}(\mathcal{E}/\hbar\omega_0 - 1)^{1/2}$; if the optical coupling is strong, $\tau_{\rm op}$ is very small and $F^+ \to \infty$. The limits (1) and (2) impose the condition

$$\mathcal{A} \gg 10.3(1/\tau_{\rm imp} + 1/\tau_{\rm ac}) \tag{4}$$

for streaming to be effective.[2] Expression (2) is easily derived by requiring that the acceleration time to reach the energy $\frac{1}{2}m^* v_0^2 = \hbar\omega_0$ [see Eq. (19)] is smaller than the inverse rate of combined impurity and acoustical-phonon scattering. Similar elementary considerations lead to (3). More accurate expressions, which consider the transition from regular, diffusive motion to streaming motion, are found in other treatments (see Ref. 4). For heavy holes in pure germanium at 4 K, one finds that $F^- = 10$ V/cm and $F^+ = 3000$ V/cm.

The aim of this article is to investigate the velocity-fluctuation noise and the diffusivity under the diffusion-to-streaming transition, when, in addition to some impurity and acoustical-phonon scattering, light-hole motion is present with concomitant interband scattering. This is an additional feature over and above the results by Bareikis *et al.*;[5] a detailed comparison with those results will be made.

II. APPROACH

The Monte Carlo method for the computation of drift velocity, mean energy, velocity-velocity correlation function, and diffusivities (transverse and longitudinal) is by now well known; see, e.g., Refs. 1 and 4–8. The frequency-dependent diffusivity for classical frequencies ($\hbar\omega \ll kT_{\rm carrier}$) is the Fourier-Laplace transform[9,10]

$$D(i\omega) = \int_0^\infty d\tau\, e^{-i\omega\tau}\langle \delta v(t)\delta v(t+\tau)\rangle , \tag{5}$$

where the angular brackets denote an ensemble average (equals time average). For quantum frequencies a Kubo-like form, valid close to thermal equilibrium, was given in Ref. 9. Far from equilibrium, the quantum correction is not known. For low frequencies or dc, as considered in this paper, Eq. (5) simply becomes

$$D=\int_0^\infty d\tau\, C(\tau)\ , \tag{6}$$

$$C(\tau)=\langle \delta v(t)\delta v(t+\tau)\rangle\ . \tag{7}$$

As we will see in the next two sections, simple analytical expressions can easily be obtained for the pure streaming regime. These can serve as a check on the detailed Monte Carlo results.

We mention here in particular that ours is a many-particle Monte Carlo procedure. An ensemble of a few thousand holes was used in the simulation, without, however, taking hole-hole scattering into account for any value of the impurity concentration. The ionized impurity concentration is denoted as N_A, though we do not necessarily exclude compensated samples. In the latter case, N_A stands for all ionized impurity species. Ionized impurity scattering was treated in the standard Conwell-Weisskopf approach with the interaction being truncated on the half of the average distance between impurities. For acoustical-phonon scattering no approximations were introduced. The optical-phonon energy $\hbar\omega_0/k$ equals 430 K. The effective masses for light and heavy holes were taken to be $m_1=0.0423$ and $m_2=0.346$, respectively, both bands being assumed parabolic. The two-hole band model is in many respects similar to the two-valley case, studied in much detail in Refs. 1 and 2. Our method followed these developments with some appropriate alterations.

In what follows we first present results for the one-band model (heavy holes only) and analytical comparisons are made (Sec. III). Next, in Sec. IV we present the full picture for the velocity autocorrelation function and the diffusivities involving light and heavy holes for fields where streaming predominates. We will observe that the effect of the added light holes on the composite picture is considerable.

III. RESULTS INVOLVING ONLY THE HEAVY-HOLE BAND

Monte Carlo results for the dependence on the electric field of the drift velocity v_d and of the mean energy $\langle \mathcal{E} \rangle$ in K are shown in Figs. 1(a) and 1(b), respectively, for three doping levels: $N_A=0$ (pure semiconductor, curves 1), $N_A=10^{20}$ m^{-3} (curves 2), and $N_A=10^{22}$ m^{-3} (curves 3). The drift velocity $v_d(F)$ shows no anomalies which

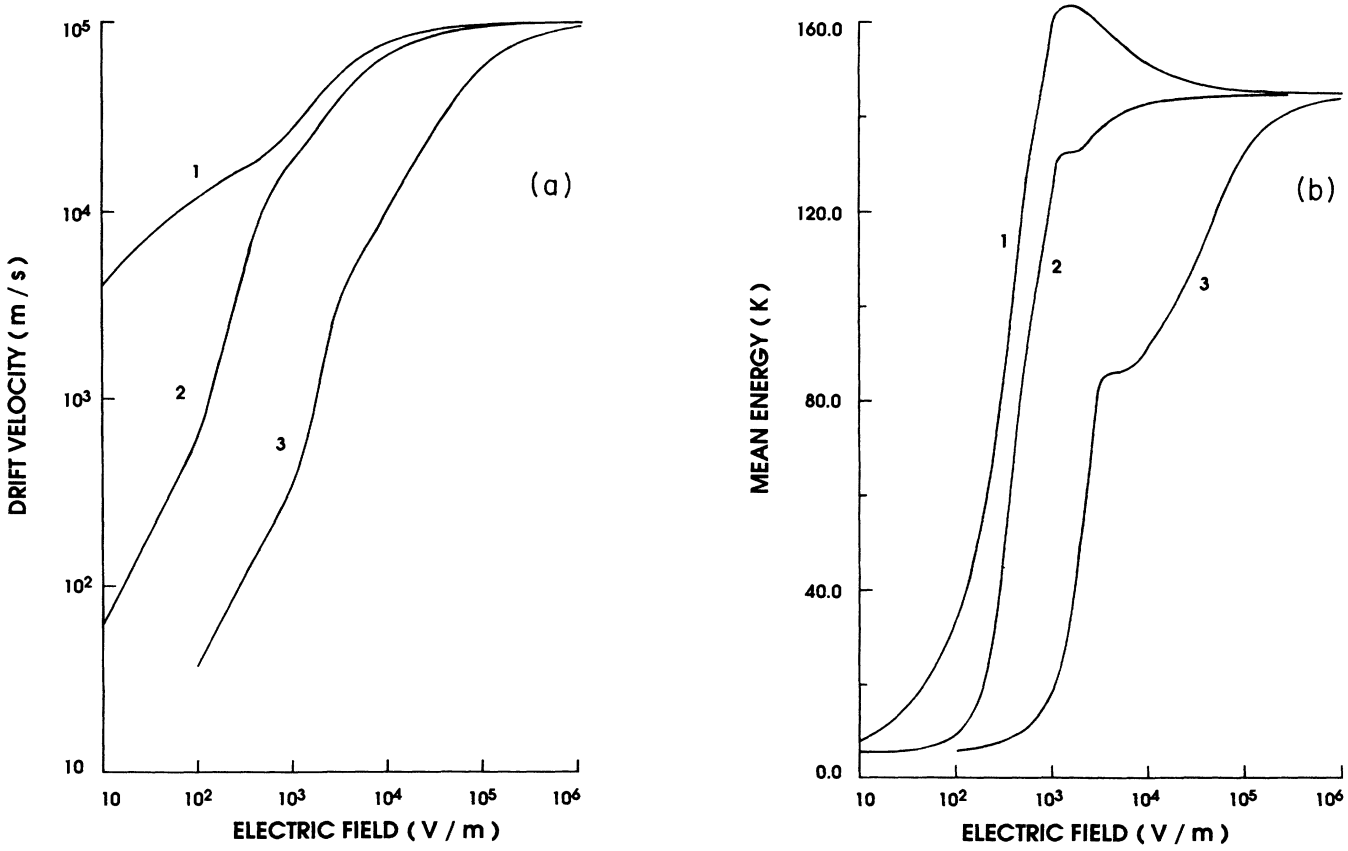

FIG. 1. (a) Field dependence of drift velocity v_d in m/s and (b) mean energy $\langle \mathcal{E} \rangle$ in K for heavy holes in a semiconductor like p-type Ge (see text) at 4 K with different ionized impurity concentrations N_A. Curve 1, $N_A=0$; curve 2, $N_A=10^{20}$ m^{-3}, curve 3, $N_A=10^{22}$ m^{-3}.

were not discussed in the literature before; the saturation value is $v_0/2$ (see below) in all three curves, where v_0 is the velocity corresponding to the energy $\mathcal{E}$ equal to $\hbar\omega_0$:

$$v_0=(2\hbar\omega_0/m_2)^{1/2} . \tag{8}$$

If streaming occurs, it is the velocity at the beginning of the active region. As to the mean energy $\langle \mathcal{E}(F) \rangle$, there is a well-pronounced maximum for the pure semiconductor, curve 1. It is due to the fact that for fields less than approximately 1000 V/m, optical-phonon emission is rare in comparison with acoustic-phonon scattering in the passive region (for example, at 500 V/m, optical-phonon emission is about 0.035% of acoustic scattering, at 10^3 V/m it becomes almost 3%, but at 5×10^3 V/m optical-phonon emission is almost equal to the rate of acoustic scattering). The mean energy therefore increases initially with F, but reaches a maximum $\langle \mathcal{E} \rangle_{\max} \simeq (9/25)\hbar\omega_0$ (Ref. 8) equal to 162 K when optical-phonon emission becomes significant; from then on the mean energy decreases due to the rapid gain in the occurrence of optical-phonon emission, to finally reach the saturation value $\hbar\omega_0/3k = 143.3$ K (see below).

When impurity scattering is added, the mean energy from the start grows less rapidly. So, the maximum which was there for $N_A=0$ no longer develops, and a quasimonotonic behavior to the saturation value is put in evidence. However, at the field where optical-phonon emission becomes sufficiently strong, a small plateau, causing a kink in the curves, appears.

The saturation values associated with streaming are easily obtained. In the simplest model for streaming, carrier velocity v and energy $\mathcal{E}=\frac{1}{2}m_2v^2$ increase with time[1-4] as ($t \le \tau_0$),

$$v=v_0(t/\tau_0), \quad \mathcal{E}=\hbar\omega_0(t/\tau_0)^2 , \tag{9}$$

where τ_0 is the time for the carrier to reach the energy $\hbar\omega_0$ from $\mathcal{E}=0$. Note that (8) and the two parts of (9) are consistent. Assuming ergodicity, the ensemble average is equal to the average over a time $N\tau_0$, $N\to\infty$, which in turn, due to the periodicity of streaming, is equal to the average over a simple period τ_0:

$$v_d=\langle v \rangle=\frac{1}{\tau_0}\int_0^{\tau_0} v_0\frac{t}{\tau_0}dt=\tfrac{1}{2}v_0 , \tag{10a}$$

$$\langle \mathcal{E} \rangle=\frac{1}{\tau_0}\int_0^{\tau_0}\hbar\omega_0\left[\frac{t}{\tau_0}\right]^2 dt=\tfrac{1}{3}\hbar\omega_0 . \tag{10b}$$

The dependences of the longitudinal and transverse diffusion coefficients $D_\parallel$ and $D_\perp$, respectively, on the electrical field are shown in Fig. 2. For the undoped semiconductor $D_\parallel$ (solid line) is smaller than $D_\perp$ (dashed line), as also observed by others[1,6] in the small electric field region. This trend reverses for $F>F_{\max}$, where $F_{\max}$ is the field corresponding to the maximum in $\langle \mathcal{E} \rangle$. Then both diffusivities decrease, going ultimately to zero. For pure streaming motion, this limiting behavior is easily understood. The transverse diffusivity goes to zero because for pure streaming the velocity component perpendicular to the electric field vanishes. The longitudinal diffusivity

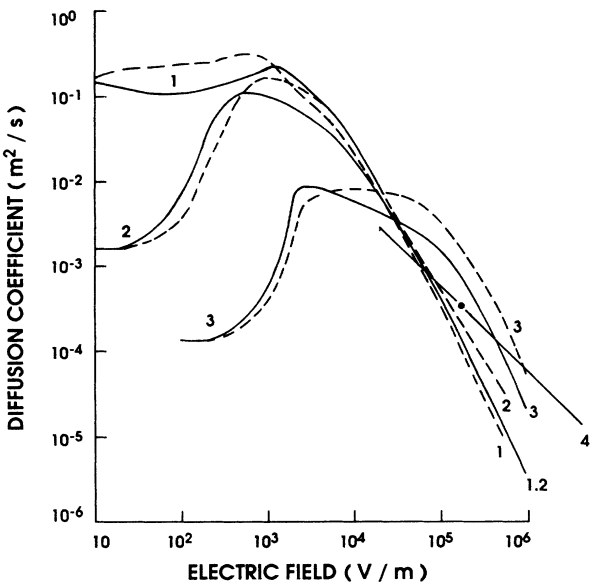

FIG. 2. Field dependence of longitudinal (solid line) and transverse (dashed line) diffusion coefficients in m^2/s for heavy holes in p-type Ge at 4 K. Curve 1, $N_A=0$; curve 2, $N_A=10^{20}$ m^{-3}; curve 3, $N_A=10^{22}$ m^{-3}. Further, curve 4 shows the result for $D_\parallel$ when light holes are added (Sec. IV).

goes to zero because the velocity-velocity correlation function becomes periodic; see below. The limiting value zero for both D's is not reached yet, however, for the fields of Fig. 2 (F up to 10^6 V/m), since acoustic-phonon scattering in the passive region was taken into account.

For the doped case ($N_A=10^{20}$ m^{-3}, curve 2, and $N_A=10^{22}$ m^{-3}, curve 3) the diffusivities are initially lower (as are the mobilities) due to added impurity scattering. However, at $F_{\max}$ (order 10^3 V/m) the curves reach a maximum and then fall off similarly as for the undoped case since we approach the conditions for pure streaming. In the high field regime, $D_\parallel$ is slightly less then $D_\perp$. Finally, curve 4 in Fig. 2 shows the influence of light-hole motion for the undoped case, as discussed in the next section. The diffusivity now falls off less rapidly; for $F \gtrsim 5\times10^4$ V/m, its value is larger than what is calculated in the one-band approximation.

We now review some analytical results for the velocity-velocity correlation function in the pure streaming limit. The velocity $v(t)$ is a periodically repeated ramp ("saw tooth" profile); for the first period, $0 \le t < \tau_0$, $v(t)$ was given by the first part of (9). For the nth period, we clearly have

$$v_n(t)=v_0[t-(n-1)\tau_0]/\tau_0, \quad (n-1)\tau_0 \le t \le n\tau_0 . \tag{11a}$$

This can, alternately, be written as

$$v_n(t)=[v_0(t/\tau_0)-(n-1)v_0][\,\Theta(t-(n-1)\tau_0) - \Theta(t-n\tau_0)] , \tag{11b}$$

where $\Theta(t)$ is the Heaviside function, $\Theta(t<0)=0$ and $\Theta(t>0)=1$ [though in (11a) we used $\le$ and $\ge$ signs, we assume in ensuing integrals that $\int_a^b dt$ means $\int_{a+0}^{b-0} dt$ to avoid ambiguity at the discontinuity of $\Theta(t)$]. From (11b) we see that for all $t \ge 0$, the velocity is represented by

$$v(t)=\sum_{n=1}^{\infty} v_n(t)=v_0(t/\tau_0)-v_0\sum_{n=1}^{\infty}\Theta(t-n\tau_0) \tag{11c}$$

[note that (11b) yields four sums; if in two of them we replace the summation index $n-1\rightarrow n$, Eq. (11c) results]. As expected, Eq. (11c) shows the periodicity

$$\begin{aligned} v(t+\tau_0)&=v_0(t/\tau_0)+v_0-v_0\sum_{n=1}^{\infty}\Theta(t-(n-1)\tau_0)\\ &=v_0(t/\tau_0)+v_0-v_0\sum_{n=0}^{\infty}\Theta(t-n\tau_0)\\ &=v_0(t/\tau_0)-v_0\sum_{n=1}^{\infty}\Theta(t-n\tau_0)=v(t)\ . \end{aligned} \tag{11d}$$

Now we find the correlation function

$$C(\tau)\equiv\langle\delta v(t)\delta v(t+\tau)\rangle=\langle v(t)v(t+\tau)\rangle-\langle v\rangle^2\ . \tag{12}$$

For $\langle v\rangle^2$ we have the value $\frac{1}{4}v_0^2$; see (10a). The ensemble average is as before replaced by a time average, which, because of periodicity, can be evaluated over a single period $0\le t\le\tau_0$. Thus for $v(t)$ we substitute the first part of (9), but for $v(t+\tau)$ we must take the full form (11c) since τ can be arbitrarily large. Hence we obtain

$$C(\tau)=\tfrac{1}{4}v_0^2\left[\int_0^{\tau_0}\frac{dt}{\tau_0}4\frac{t}{\tau_0}\left[\frac{t+\tau}{\tau_0}-\sum_{n=1}^{\infty}\Theta(t+\tau-n\tau_0)\right]-1\right]\ . \tag{13}$$

The following identity is easily established for any $\phi(t)$:

$$\int_0^{\tau_0}dt\,\phi(t)\Theta(t+\tau-n\tau_0)=\int_0^{\tau_0}dt\,\phi(t)\Theta(\tau-n\tau_0)+\int_{n\tau_0-\tau}^{\tau_0}dt\,\phi(t)[\Theta(\tau-(n-1)\tau_0)-\Theta(\tau-n\tau_0)]\ ; \tag{14}$$

the first part only survives if $\tau>n\tau_0$ and the second part describes the result for $\tau<n\tau_0$, in addition to $n\tau_0-\tau<\tau_0$. Thus, for $C(\tau)$ one easily finds

$$\begin{aligned} C(\tau)&=\tfrac{1}{4}v_0^2\left\{\tfrac{1}{3}+2\frac{\tau}{\tau_0}-2\sum_{n=1}^{\infty}\Theta(\tau-n\tau_0)-2\sum_{n=1}^{\infty}\left[1-\left[n-\frac{\tau}{\tau_0}\right]^2\right][\Theta(\tau-(n-1)\tau_0)-\Theta(\tau-n\tau_0)]\right\}\\ &=\tfrac{1}{12}v_0^2\left[1-6\frac{\tau}{\tau_0}\left[1-\frac{\tau}{\tau_0}\right]-12\sum_{n=1}^{\infty}\left[\frac{\tau}{\tau_0}-n\right]\Theta(\tau-n\tau_0)\right] \end{aligned} \tag{15}$$

[to obtain this result it is only necessary to change $n-1\rightarrow n$ in the sum involving $\Theta(\tau-(n-1)\tau_0)$ and split off the term with $n=0$]. *The above is the complete result for all* τ. One easily establishes the periodicity expected:

$$\begin{aligned} C(\tau+\tau_0)&=\tfrac{1}{12}v_0^2\left\{\left[1-6\left[\frac{\tau}{\tau_0}+1\right]+6\left[\frac{\tau}{\tau_0}+1\right]^2\right]-12\sum_{n=0}^{\infty}\left[\frac{\tau}{\tau_0}-n\right]\Theta(\tau-n\tau_0)\right\}\\ &=\tfrac{1}{12}v_0^2\left\{\left[1-6\left[\frac{\tau}{\tau_0}+1\right]+6\left[\frac{\tau}{\tau_0}+1\right]^2\right]-12\left[\frac{\tau}{\tau_0}\right]-12\sum_{n=1}^{\infty}\left[\frac{\tau}{\tau_0}-n\right]\Theta(\tau-n\tau_0)\right\}\\ &=C(\tau)\ . \end{aligned} \tag{16}$$

We notice that (15) is a periodically repeated parabola. For the first period, $0\le\tau\le\tau_0$, one finds with $\tau/\tau_0=y$

$$C_1(\tau)=\tfrac{1}{12}v_0^2[1-6y(1-y)]\ . \tag{17a}$$

Likewise, with minor algebra, for the second period $\tau_0\le\tau<2\tau_0$ if $\tau/\tau_0=1+\bar{y}$, or $\bar{y}=(\tau-\tau_0)/\tau_0$,

$$C_2(\tau)=\tfrac{1}{12}v_0^2[1-6\bar{y}(1-\bar{y})]\ , \tag{17b}$$

etc. The parabola is invariant for the substitution $y\rightarrow 1-y$. For $\tau=0$ and $\tau=\tau_0$, the normalized value $C^*(\tau)=C(\tau)/v_d^2$ equals 0.333; the minimum, occurring at $\tau=\frac{1}{2}\tau_0$, yields for $C^*(\tau)$ the value -0.166. Finally, for the diffusivity we obtain the result

$$\begin{aligned} \mathcal{D}_{\parallel}&=\lim_{T\rightarrow\infty}\int_0^T C(\tau)d\tau\\ &=\lim_{N\rightarrow\infty}(Nv_0^2\tau_0/12)\int_0^1 dy\,[1-6y(1-y)]\\ &=0 \end{aligned} \tag{18}$$

providing the limit $T\sim N\tau_0\rightarrow\infty$ is taken *a posteriori* (in any practical situation the sampling time is always finite; more on this below).

We now turn to the Monte Carlo results. In Figs. 3–5 the normalized autocorrelation function $C^*(\tau)$ is presented for a very low field $F=500$ V/m (Fig. 3), for an intermediate field $F=5000$ V/m (Fig. 4), and for a high field $F=5\times10^4$ V/m [Figs. 5(a)–5(c)]. In all figures curve 1 represents the Monte Carlo computation if acoustic-phonon as well as impurity scattering was assumed to be

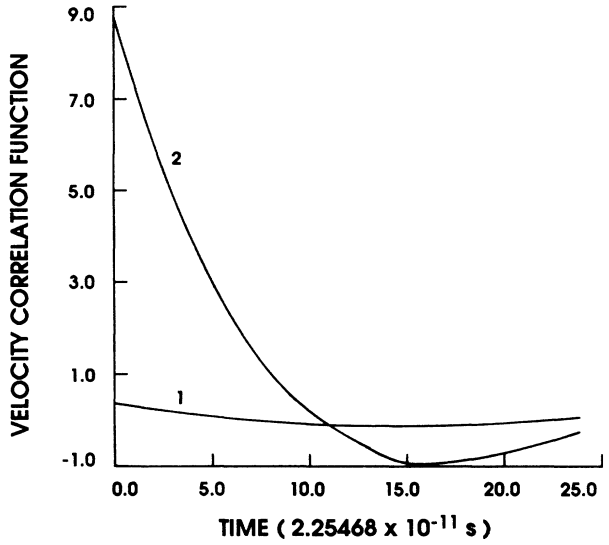

FIG. 3. Normalized velocity-velocity correlation function $C^*(t)$ for heavy holes in p-type Ge at 4 K for $F=500$ V/m. Curve 1, streaming only; curve 2, including acoustical-phonon scattering.

absent, as in the theoretical considerations on the streaming motion behavior. On the contrary, in curves 2 we took acoustic-phonon scattering in the passive region into account (but not ionized impurity scattering, corresponding to the $N_A=0$ curves in Figs. 1 and 2). So these curves represent more properly the transition from diffusive motion to streaming behavior. As indicated above, $C^*(\tau)=C(\tau)/v_d^2$. For pure streaming, $v_d=v_0/2$ is independent of the electrical field; see Eq. (8). With $\hbar\omega_0$ given before, we obtained $v_d=9.7\times10^4$ m/s. If

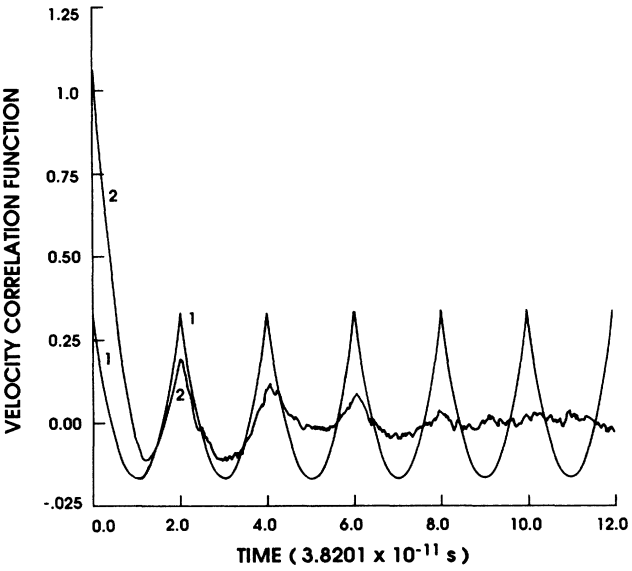

FIG. 4. Normalized velocity-velocity correlation function $C^*(t)$ for heavy holes in p-type Ge at 4 K for $F=5000$ V/m. Curve 1, streaming only; curve 2, including acoustical-phonon scattering.

acoustic-phonon scattering is taken into account, we find $v_d=2.074\times10^4$ m/s for $F=500$ V/m, $v_d=6.74\times10^4$ m/s for $F=5000$ V/m, and $v_d=9.47\times10^4$ m/s for $F=5\times10^4$ V/m. The latter is close to the pure streaming limit value. We now discuss these figures in more detail.

In Fig. 3, dealing with $F=500$ V/m, the time τ_0 is quite long. From (9) and (8) one easily sees that

$$\tau_0=m_2v_0/eF=(2\hbar\omega_0m_2)^{1/2}/eF\ . \tag{19}$$

From this one obtains $\tau_0=7.64\times10^{-10}$ s. In Fig. 3 this corresponds to approximately 34 units on the indicated time scale. Thus the 25 units shown in the figure cover about 73% of the first streaming interval. The structure of the parabola is weakly discernable in curve 1. Realistically, however, curve 2 shows the expected behavior. Since only 0.035% of the scattering involves optical-phonon emission, as indicated by the low value of v_d, $C^*(\tau)$ is quite different; its initial value is positive and large, whereas for $\tau\approx\frac{1}{2}\tau_0$ it is more negative than for curve 1. With the time the amplitude of the fluctuations of $C^*(\tau)$ decreases so that $C^*(\tau)$ tends towards zero.

In Fig. 4 the field is a factor 10 higher, leading to $\tau_0=7.6402\times10^{-11}$ s. The periodic streaming motion in curve 1 is clearly visible. The peaks have the value $C^*=0.333$ and the minima are -0.166 in agreement with the analytical results. This curve is therefore a strong verification for the algorithm used in the MC procedure. Curve 2 takes acoustic-phonon scattering in the passive region into account and is essentially the same as Fig. 4 in Ref. 5 by Bareikis *et al.* We notice that streaming motion develops but only 4 periods are clearly visible. For longer times it rapidly damps out due to the fact that at the end of each period only a fraction of the holes reach the velocity $v(\tau_0)=v_0$, so the conditional ensemble average $\langle v(\tau_0)|v(0)\rangle$ is less than v_0; the cumulative effect then gives diminishing correlation, since by Bayes' theorem

$$\langle v(\tau_0)v(0)\rangle=\langle\langle v(\tau_0)|v(0)\rangle v(0)\rangle<\langle v_0v(0)\rangle$$

$$=\langle v(\tau_0)v(0)\rangle_{\rm str}\ . \tag{20}$$

All this is more strongly visible in Figs. 5(a)–5(c). The streaming period τ_0 is now 7.6402×10^{-12} s. Figure 5(a) covers the first 5 periods; in Fig. 5(b) the behavior after 20 and up to 25 periods is shown, while in Fig. 5(c) the "asymptotic" trends for periods 55–60 are indicated. The streaming curves (curves 1) are again as expected, showing the oscillatory parabolic behavior *ad infinitum*. The more realistic behavior (curves 2) follows the pure streaming case quite closely for the first 5 periods, as seen in Fig. 5(a). This is because there is only one acoustical scattering event (on the average) for five optical-phonon emissions. Then, for periods 20–25 [Fig. 5(b)], the damping has again been appreciable; the streaming periodicity is still here, but the maxima and minima have diminished. Finally, as Fig. 5(c) shows, the correlation has damped out and the stationary correlation function $\langle\delta v(\tau)\delta v(0)\rangle$ hovers around the value zero.

In the preceding discussion we assumed ergodicity, i.e.,

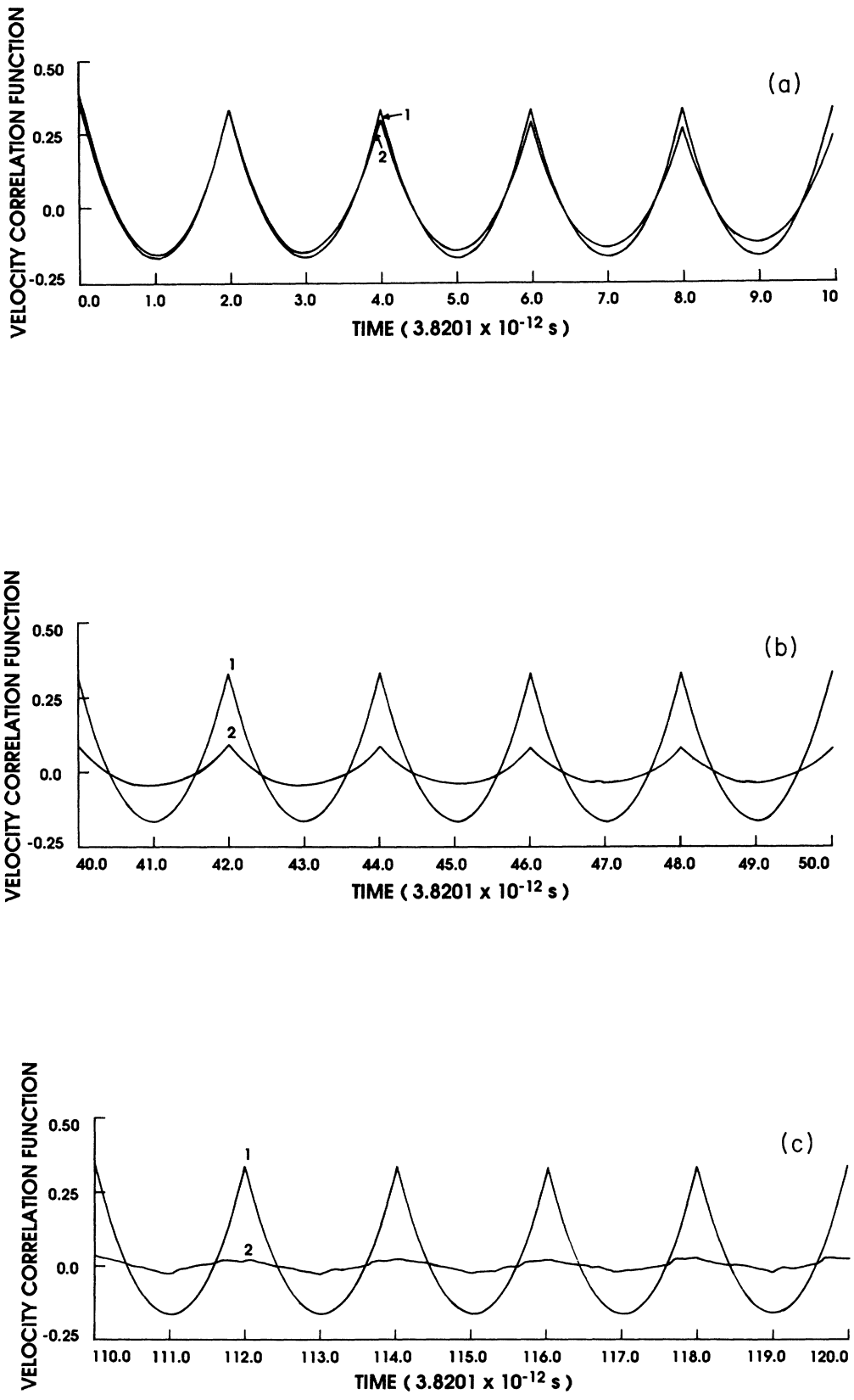

FIG. 5. Normalized velocity-velocity correlation function $C^*(t)$ for heavy holes in p-type Ge at 4 K for $F=5\times10^4$ V/m. Curve 1, pure streaming; curve 2, acoustical-phonon scattering added. (a) first 5 periods, (b) periods 20–25, and (c) 55–60.

equivalence of ensemble and time averages. As Fig. 5(c) shows, for the time average to be valid a finite time suffices. Notice that the real time $T \simeq 5\times 10^{-10}$ s suffices to find the time average for any electric field, but the dimensionless time, $N = T/\tau_0$, where τ_0 is the streaming period, must increase when the electric field increases. The same holds for the time T involved in $D \sim \int_0^T C(\tau)d\tau$, in order for convergence to occur and D to be meaningful.

IV. RESULTS INCLUDING THE MOTION OF LIGHT HOLES AND INTERBAND SCATTERING

The motion of the light holes is similar to that for the heavy holes. For pure streaming, the equations of the previous section, with m_2 replaced by m_1, apply. The diffusion coefficient of the streaming motion is likewise zero. The transit period to reach the energy $\hbar\omega_0$ is shorter since the mass is smaller. As in (19) we have

$$\tau_{02} = (2\hbar\omega_0 m_2)^{1/2}/eF \ , \tag{19'}$$

$$\tau_{01} = (2\hbar\omega_0 m_1)^{1/2}/eF = \sqrt{\gamma}\,\tau_{02} \ ,$$

where $\gamma = m_1/m_2$. The drift velocities for the two bands are [see (8)]

$$\langle v_2 \rangle \equiv v_{d2} = \tfrac{1}{2} v_{02} = (\hbar\omega_0/2m_2)^{1/2} \ , \tag{21a}$$

$$\langle v_1 \rangle \equiv v_{d1} = \tfrac{1}{2} v_{01} = (\hbar\omega_0/2m_1)^{1/2} = \langle v_2 \rangle/\sqrt{\gamma} \ . \tag{21b}$$

When a heavy hole is accelerated to v_{02} it emits an optical phonon and it may then stay in the heavy-hole band or be scattered to the light-hole band, in accordance with the density of states in these bands.[11,12] The interband scattering times, denoting by τ_2 the scattering time from the heavy-hole band to the light-hole band and by τ_1 the scattering time from the light- to heavy-hole band, are very simple for the streaming case; they are given by

$$\tau_2 = \tau_{02}\gamma^{-3/2}(1+\gamma^{3/2}), \quad \tau_1 = \tau_{01}(1+\gamma^{3/2}) \ . \tag{22}$$

We also introduce the relaxation time

$$\frac{1}{\tau} = \frac{1}{\tau_1} + \frac{1}{\tau_2} = \frac{1}{\tau_{02}} \frac{(1+\gamma^2)}{\sqrt{\gamma}(1+\gamma^{3/2})} \ . \tag{23}$$

The only observable diffusivity in the absence of acoustical-phonon and impurity scattering is due to the interband scattering. For this we have the well-known result[13]

$$D_\parallel = \nu_1\nu_2(\langle v_1 \rangle - \langle v_2 \rangle)^2\tau \ , \tag{24}$$

where ν_1 and ν_2 are the fractions of holes in the two bands. From detailed balance

$$\nu_1/\tau_1 = \nu_2/\tau_2 \quad \text{and} \quad \nu_1+\nu_2 = 1 \tag{25}$$

we have

$$\nu_1 = \tau/\tau_2, \quad \nu_2 = \tau/\tau_1 \ . \tag{26}$$

Substituting (21b), (22), (23), and (26) into (24) we then obtain

$$D_\parallel = \langle v_2 \rangle^2 \tau_{02} \frac{\gamma^{3/2}(1-\sqrt{\gamma})^2(1+\gamma^{3/2})}{(1+\gamma^2)^3} \ . \tag{27}$$

With the effective masses given in Sec. II and the expressions (19') and (21a) for τ_{02} and $\langle v_2 \rangle$, one finds (in m^2/s)

$$D_\parallel = 64.5/F \ , \tag{28}$$

F in V/m. The dependence on F of this $D_\parallel$ was given by curve 4 in Fig. 2. For rather pure samples ($N_A \lesssim 10^{20}/m^3$) the interband diffusion coefficient predominates for fields larger than 10^5 V/m. Below we will see that already for lower fields the correlation function is drastically altered by the addition of light-hole motion.

More detail is revealed by the MC computation of the normalized velocity-velocity correlation function $C^*(\tau) = C(\tau)/\langle v_2 \rangle^2$. Figures 6(a)–6(d), all referring to a field of 5×10^4 V/m, give the results for several time intervals [Fig. 6(a), up to 5 periods; Fig. 6(b), periods 20–25; Fig. 6(c), periods 55–60; Fig. 6(d), periods 115–120]. The total time covered is $\approx 10^{-9}$ sec. (For lower fields, similar results have been found when the time period is correspondingly increased). Curve 1 is again the result for pure streaming when only heavy holes are present; the field being 5×10^4 V/m, one finds for the transit time of the passive region $\tau_{02} = 7.6402\times 10^{-12}$ s. These curves are therefore the same parabolas as seen in Fig. 5. Then curves 2 show the results when both light and heavy holes are present.

Though the light-hole contribution to transport is discussed in various papers (see, e.g., Refs. 6 and 14), we are not aware of any papers discussing the light-hole contribution to the diffusivity under streaming motion. Figure 6(a) reveals that the first 5 periods do not cause too much of a change. However, the contribution of the light holes causes a kink with a slight maximum to appear. After 20 periods, Fig. 6(b), the maxima of the original parabolas are considerably decreased due to transfer of heavy holes to the light-hole band. Also, the period τ_0 is more or less divided into three parts; two submaxima have developed. This is even more pronounced for larger times, see Figs. 6(c) and 6(d). The submaxima are most likely associated with heavy holes which are scattered twice to the other band or back. We notice that the interband scattering time is related to τ_{02} [see Eq. (23)] by the fraction $\sqrt{\gamma}(1+\gamma^{3/2})/(1+\gamma^2)$, which is very close to $\frac{1}{3}$. That is why the oscillations with about $\tau_0/3$ develop; because the factor τ/τ_{02} is not exactly $\frac{1}{3}$, however, a small gradual shift occurs as is seen by comparing Fig. 6(c) with Fig. 6(d). In the latter picture a stationary periodicity has developed which, in contrast to the effect of acoustical-phonon scattering, shows no sign of damping out. So for $\tau \gg \tau_0$ there is no contribution of $C(\tau)$ to the diffusivity $D_\parallel$. Altogether, however, the presence of light holes and interband scattering drastically alters the correlation function under otherwise "pure" streaming conditions.

To conclude, we want once more to stress the major result of our calculations. For this purpose, let us write the expression for the average drift velocity, $\langle v \rangle = v_d$, for a two-band semiconductor. From (21) and (26) it follows that

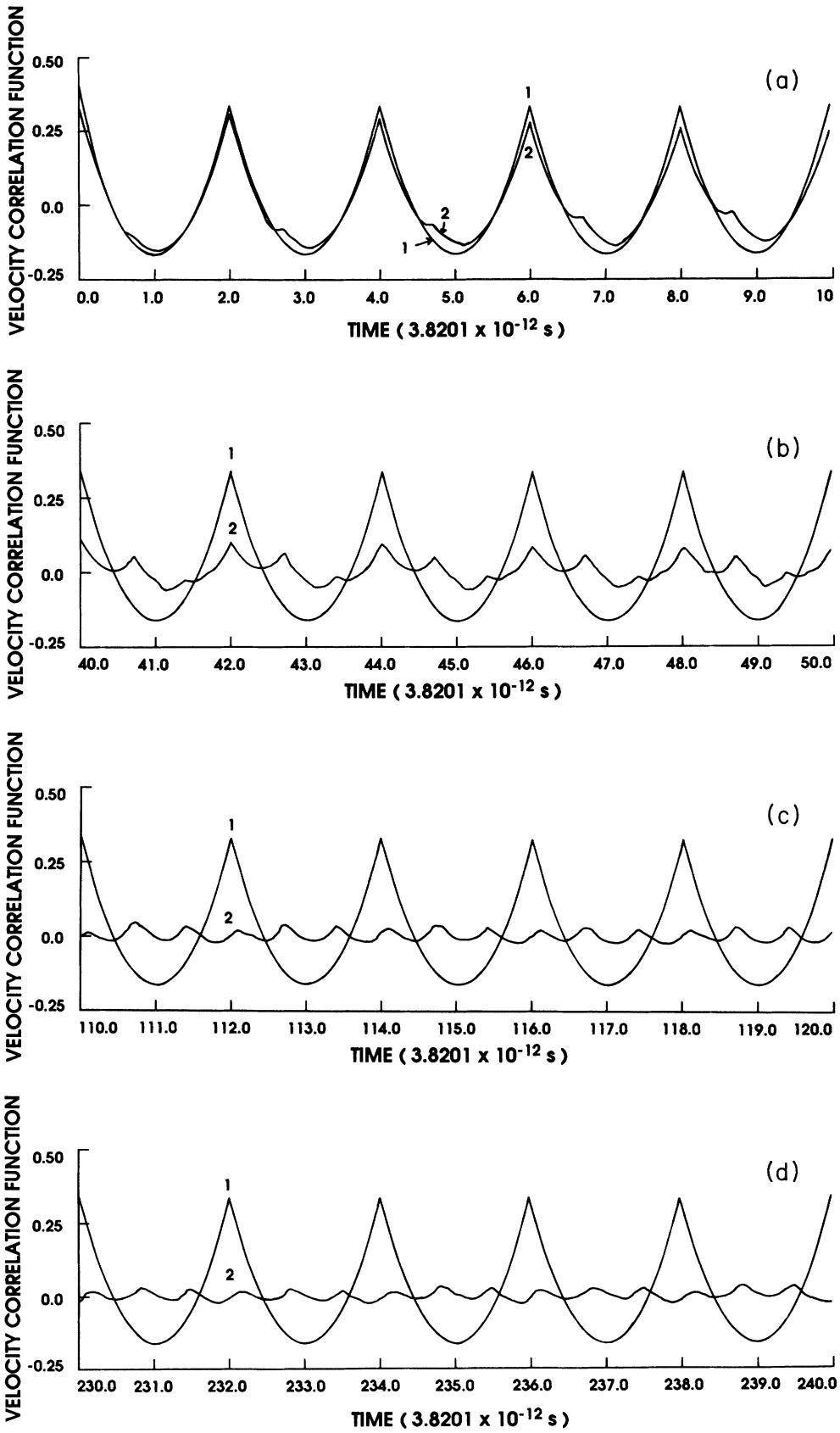

FIG. 6. Normalized velocity-velocity correlation function $C^*(t)$ for hole motion in p-type Ge at 4 K for $F=5\times10^4$ V/m. Curve 1, heavy-hole motion only; curve 2, effect of light-hole motion and interband scattering. (a) first 5 periods, (b) periods 20–25, (c) periods 55–60, and (d) periods 115–120.

$$\langle v \rangle = v_d = \nu_1 v_{d1} + \nu_2 v_{d2} = v_{d2}(1+\gamma^{3/2})/(1+\gamma^2) = 1.027\,39 v_{d2}\ , \quad (29)$$

where we take into account the value of $\gamma = 0.122\,25$. So we have encountered the very special situation in which the longitudinal diffusion coefficient [see Fig. 2 and Eqs. (27) and (28)], as well as the velocity-velocity correlation function (see Fig. 6), changes drastically, but the average drift velocity [(29)] remains almost the same when, in addition to the heavy holes, the light holes are taken into account. The peculiarity is in the streaming motion (or close to streaming motion), when a carrier can emit an optical phonon several times before any other scattering in the passive region occurs; this situation was discussed in detail in our paper.

But let us now come back to the results of previous publications,[6,12,14–16] where transport in p-type semiconductors was studied taking into account the contributions from both bands. In the above papers and in other publications, the main attention was paid to the importance of interband scattering by acoustic phonons. In all these cases, the ratio of the light- to the heavy-hole concentration was equal or less than the corresponding ratio of the density of states in the bands, i.e., $\nu_1/\nu_2 \leq \gamma^{3/2}$ [in our case, $\nu_1/\nu_2 = \gamma^2$, see Eqs. (26), (22), and (19′)]. As soon as the average probability of scattering of a light hole to the heavy-hole band due to the interaction with the acoustic phonons equals the intraband scattering of heavy holes, the average drift velocity of the light holes is higher than that of the heavy holes due to the difference in the effective masses, so $v_{d1} \leq v_{d2}/\gamma$ (in our case $v_{d1} = v_{d2}/\sqrt{\gamma}$). So the contribution of light holes to the average drift velocity can be proportional to $\sqrt{\gamma}$, i.e., $v_d \leq v_{d2}(1+\sqrt{\gamma})/(1+\gamma^{3/2})$ [compare with (29)]. If we use our value of γ, we can easily see that instead of v_{d2} for the one-band approach, we can get $1.29 v_{d2}$ for the two-band approach. The coupling of heavy- and light-hole bands via acoustic-phonon scattering gives a contribution to the noise of the same order of magnitude as the noise calculated for the heavy-hole band only, and this is analogous to the additional contribution to the average drift velocity. We have not discussed this in the paper since from our point of view this is an obvious result, which is always automatically present in Monte Carlo simulations. Instead of that, we considered the condition when the acoustic-phonon scattering became unimportant. Due to this, the diffusion coefficient of the heavy holes tends to zero for close to streaming motion, so that only diffusion due to the interband scattering (24) remains.

ACKNOWLEDGMENTS

This research was sponsored in part by the Natural Sciences and Engineering Research Council of Canada under Grant A-9522. This research was supported in part by FCAR (Québec).

*On leave from the Institute of Semiconductors of the Academy of Sciences of the Ukrainian S.S.R. Prospect Nauki 45, 252 650 Kiev, U.S.S.R.

[1] *Hot Electron Transport in Semiconductors,* edited by L. Reggiani (Springer-Verlag, Berlin, 1985).

[2] S. Komigama, Adv. Phys. **31**, 255 (1982).

[3] *Striming i Anizotropnij Raspredelenija v Skreshchenich Polijach,* edited by A. A. Andronov and J. K. Pozela (Nauka, Gorkij, 1983).

[4] F. M. Peters, W. Van Puymbroeck, and J. T. Devreese, Phys. Rev. B **31**, 5322 (1985).

[5] V. Bareikis, A. Galdikas, R. Miliušytė, and V. Viktoravičius, in *Proceedings of the Sixth International Conference on Noise in Physical Systems,* Natl. Bur. Stand. (U.S.) Spec. Publ. No. 614, edited by P. H. E. Meijer, R. D. Mountain, and R. J. Soulen (U.S. GPO, Washington, D.C., 1981), p. 406.

[6] C. Jacoboni and L. Reggiani, Rev. Mod. Phys. **55**, 645 (1983).

[7] R. Brunetti and C. Jacoboni, Phys. Rev. Lett. **50**, 1164 (1983); Phys. Rev. B **29**, 5739 (1984).

[8] V. A. Kochelap, V. Mitin, and N. A. Zakhleniuk, Zh. Expt. Theor. Fiz. **95**, 1495 (1989) [Sov. Phys.—JETP **68**, 863 (1989)].

[9] K. M. Van Vliet and A. van der Ziel, Physica **99A**, 337 (1979).

[10] R. Kubo, J. Phys. Soc. Jpn. **12**, 570 (1957).

[11] M. Costalo and L. Reggiani, Phys. Status Solidi B **58**, 461 (1973).

[12] G. L. Bir and G. E. Pikus, Fiz. Tverd. Tela (Leningrad) **1**, 1642 (1959) [Sov. Phys.—Solid State **1**, 1502 (1960)]; **2**, 2287 (1960) [**2**, 2039 (1961)].

[13] R. Brunetti, C. Jacoboni, and L. Reggiani, J. Phys. (Paris) Colloq. **42**, C7-117 (1981).

[14] V. M. Ivashchenko, V. V. Mitin, and N. A. Zakhleniuk, Phys. Status Solidi B **115**, 245 (1983).

[15] S. Bosi, C. Jacoboni, and L. Reggiani, J. Phys. C **12**, 1525 (1979).

[16] V. V. Mitin, Fiz. Tekh. Poluprovodn. **9**, 1413 (1975) [Sov. Phys.—Semicond. **9**, 932 (1975)]; **10**, 1562 (1976) [**10**, 928 (1976)].